

Marquette University

**e-Publications@Marquette**

***Electrical and Computer Engineering Faculty Research and Publications/College of Engineering***

***This paper is NOT THE PUBLISHED VERSION; but the author's final, peer-reviewed manuscript. The published version may be accessed by following the link in the citation below.***

*Proceedings of SPIE 8973: Micromachining and Microfabrication Process Technology XIX*, No. 8973 (March 2014). [DOI](#). This article is © Society of Photo-optical Instrumentation Engineers (SPIE) and permission has been granted for this version to appear in [e-Publications@Marquette](mailto:e-Publications@Marquette). Society of Photo-optical Instrumentation Engineers (SPIE) does not grant permission for this article to be further copied/distributed or hosted elsewhere without the express permission from Society of Photo-optical Instrumentation Engineers (SPIE).

# Optimal Microelectromechanical Systems (MEMS) Device for Achieving High Pyroelectric Response of AlN

Bemnet Kebede

Air Force Institute of Technology

Ronald A. Coutu

Air Force Institute of Technology

LaVern Starman

Air Force Research Lab.

## Abstract

This paper discusses research being conducted on aluminum nitride (AlN) as a pyroelectric material for use in detecting applications. AlN is being investigated because of its high pyroelectric coefficient, thermal stability, and high Curie temperature. In order to determine suitability of the pyroelectric properties of AlN for use as a detector, testing of several devices was conducted. These devices were fabricated using microelectromechanical systems (MEMS) fabrication processes; the devices were also

designed to allow for voltage and current measurements. The deposited AlN films used were 150 nm – 300 nm in thickness. Thin-films were used to rapidly increase the temperature response after the thermal stimulus was applied to the pyroelectric material. This is important because the pyroelectric effect is directly proportional to the rate of temperature change. The design used was a face-electrode bridge that provides thermal isolation which minimizes heat loss to the substrate, thereby increasing operation frequency of the pyroelectric device. A thermal stimulus was applied to the pyroelectric material and the response was measured across the electrodes. A thermal imaging camera was used to monitor the changes in temperature. Throughout the testing process, the annealing temperatures, type of layers, and thicknesses were also varied. These changes resulted in improved MEMS designs, which were fabricated to obtain an optimal design configuration for achieving a high pyroelectric response. A pyroelectric voltage response of 38.9 mV<sub>p-p</sub> was measured without filtering, 12.45 mV<sub>p-p</sub> was measured in the infrared (IR) region using a Si filter, and 6.38 mV<sub>p-p</sub> was measured in the short wavelength IR region using a long pass filter. The results showed that AlN's pyroelectric properties can be used in detecting applications.

## 1. INTRODUCTION

The interest in the pyroelectric properties of various materials has increased since the early 1960s when J. Cooper looked at the practical application of pyroelectric radiation detectors.<sup>1</sup> The increased interest in pyroelectricity after the 1960s may incorrectly lead one to infer that the subject of pyroelectricity is relatively new, although interest in pyroelectricity has existed for many years. In fact, the pyroelectric effect was seen as early as 300 BC by the Greek philosopher, Theophrastus, who described, in his book, *On Stones*, a stone that would attract wood particles and small pieces of straw when heated.<sup>2</sup> It is believed that the stone he described, *lyngourion* in Greek, was the mineral tourmaline, and that those attractions were due to electrostatic charges built up as a result of the temperature change.<sup>3</sup> While there was interest in pyroelectricity in Theophrastus's time, it focused on the origins of the stone and whether or not it possessed therapeutic properties.<sup>3</sup>

Pyroelectricity is the temperature dependence of the spontaneous polarization of certain anisotropic solids.<sup>3</sup> In other words, a material is said to be pyroelectric if it exhibits spontaneous polarization as a result of thermal stimulus such that:

$$i_p = Ap \frac{dT}{dt} \quad (1)$$

where  $i_p$  is the pyroelectric current,  $A$  is the area of the detector,  $p$  is the pyroelectric coefficient and  $dT/dt$  is the rate of change of the temperature with respect to time.<sup>4</sup>

This fact makes pyroelectric materials uniquely suited to be used as thermal sensors because they develop a polarization when thermal stimulus is applied to them.<sup>5</sup> A distinct advantage of pyroelectric detectors over other types of thermal detectors is that pyroelectric detectors do not require cryogenic cooling. Additionally, pyroelectric detectors are sensitive over a large spectral bandwidth, have low power requirements, exhibit fast responses, and are relatively cheap to manufacture.<sup>3</sup>

## 2. DESIGN

As discussed in the introduction, the pyroelectric response is directly proportional to the rate of change in temperature. Therefore, it was necessary to design a structure that would allow for

measurements of the pyroelectric response while a thermal stimulus was being applied to the pyroelectric material. The design incorporated a face-electrode configuration and a bridge structure. The face-electrode configuration is simply two electrodes sandwiching the pyroelectric material forming a parallel plate capacitor with the thermal radiation incident on the face of the electrode versus an edge-electrode configuration where the electrodes are placed on the edges, parallel to thermal radiation.<sup>6</sup> A simple example of the face-electrode and edge electrode configurations can be seen in **Figure 1**.

**Figure 1.** (a) Face-electrode configuration, where the shaded region represents the top electrode. (b) Edge-electrode configuration where the shaded regions represent the electrodes. Modified from.<sup>6</sup>

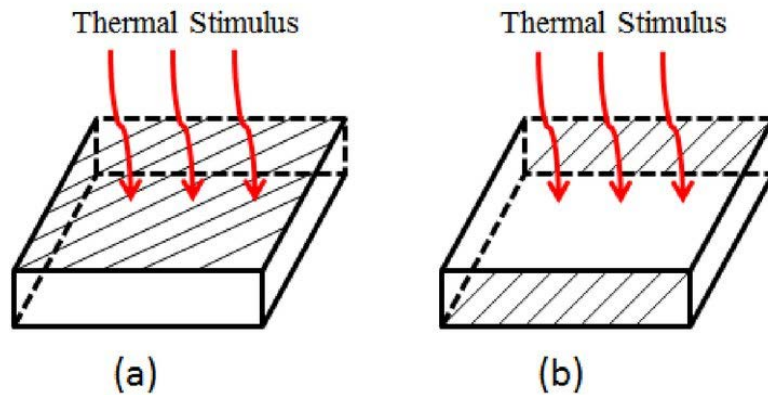
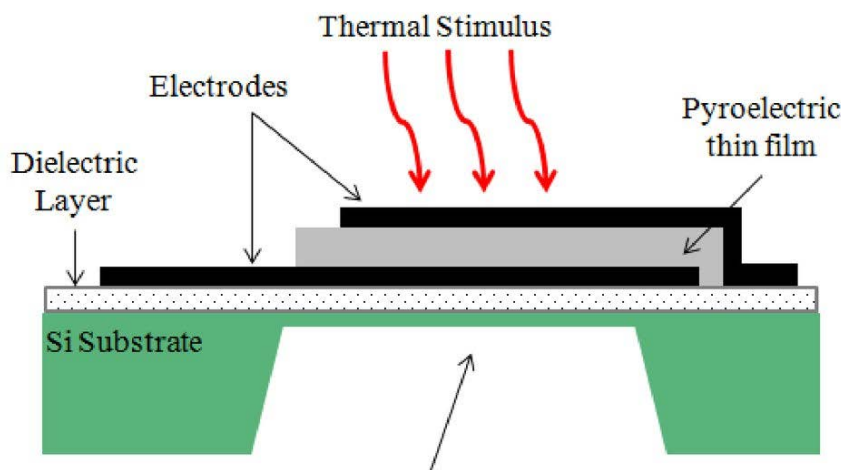


**Figure 2** shows the design structure chosen for this research. This bridge structure using the face-electrode configuration, where the electrodes are perpendicular to thermal stimulus, was chosen because it offers thermal isolation under the entire pyroelectric material which minimizes heat loss to the substrate. This structure has electrode placement on the more supportive part of the structure, allowing for probe placement without destroying the device, and is easier to fabricate than a micromachined air gap.

**Figure 2.** Pyroelectric bridge test structure used to measure pyroelectric voltage response. The bridge structure has a large air gap in the substrate for thermal isolation. Modified from.<sup>4</sup>

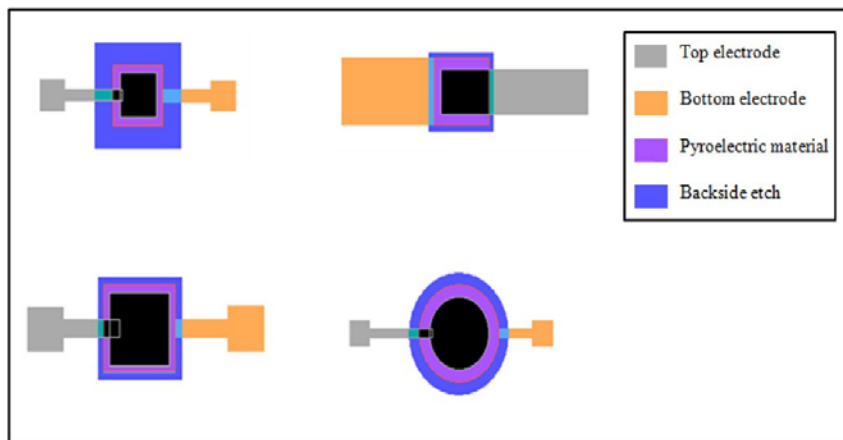


MEMSPRO software was used to layout the pyroelectric devices. Four different mask sets were created, one mask for each layer: bottom electrode, pyroelectric material, top electrode, and one for the backside etch. Utilizing a bridge design discussed earlier, four different designs were created. The electrodes are different sizes and the pyroelectric materials are also different in size and geometrical

shape. However, only one of these designs was used for this part of this research and all of the measurements discussed were from these devices. The devices used were square devices with a pyroelectric layer that was  $300 \times 300 \mu\text{m}^2$  in area.

**Figure 3** shows the four different designs that were created as they appeared in the MEMSPro software. The gray and orange arms were the electrodes, the light purple was the pyroelectric material layer, and the dark purple represented the area being etched away on the backside to create the thermal isolation.

**Figure 3.** MEMSPro software was used to layout the pyroelectric devices. The gray and orange arms represent the top and bottom electrodes, the light purple is the pyroelectric material layer, and the dark purple is the backside etch area.

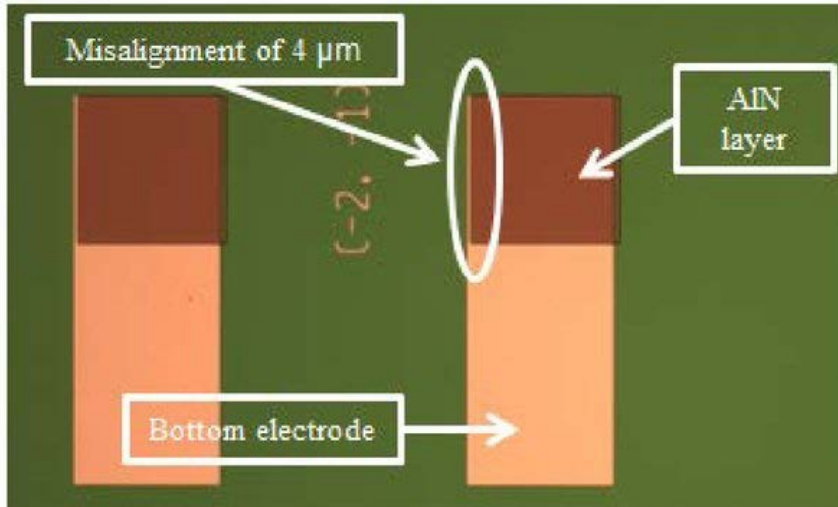


### 3. FABRICATION

The devices described in the previous section were created using MEMS fabrication processes. This section will describe the main processes used to fabricate these devices.

First the dielectric layer was deposited using plasma-enhanced chemical vapor deposition (PECVD). For this research, 250 nm of silicon nitride ( $\text{Si}_3\text{N}_4$ ) was deposited as the dielectric layer. The bottom electrode was then patterned using the bottom electrode mask for deposition of approximately 250 nm of Au. After the liftoff method was performed to remove the unwanted Au, the pyroelectric mask was used to pattern the pyroelectric layer. 300 nm of AlN was deposited using RF sputtering. **Figure 4** shows the misalignment of the pyroelectric material on top of the bottom electrode for one test structures. This misalignment could have resulted in a short circuit if the top electrode made contact with the bottom electrode.

**Figure 4.** Microscope image of AlN layer (dark brown) misaligned by 4  $\mu\text{m}$  on top of Au bottom electrode.



The top electrode deposition was accomplished using the same steps performed in the bottom electrode deposition process. Lastly, the backside etch is patterned and a deep reactive ion etch (DRIE), which etched away the areas on the backside of the substrate, was performed. DRIE is used to form high aspect ratio structures.<sup>7</sup> **Figure 5** shows the backside of a wafer after it was patterned and a closer view after the DRIE was performed.

**Figure 5.** Picture (left) of the backside of a 2 inch wafer before the backside etch was completed. The image on the right is a microscope picture that provides a closer view of the area inside of the rectangle in the picture on the left after being etched.

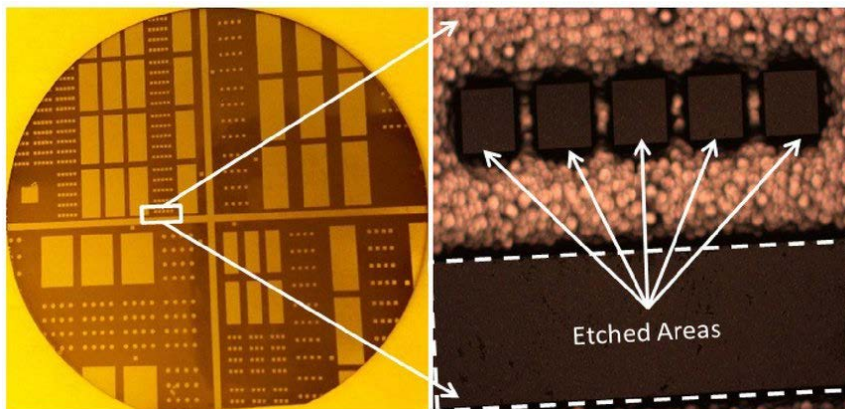
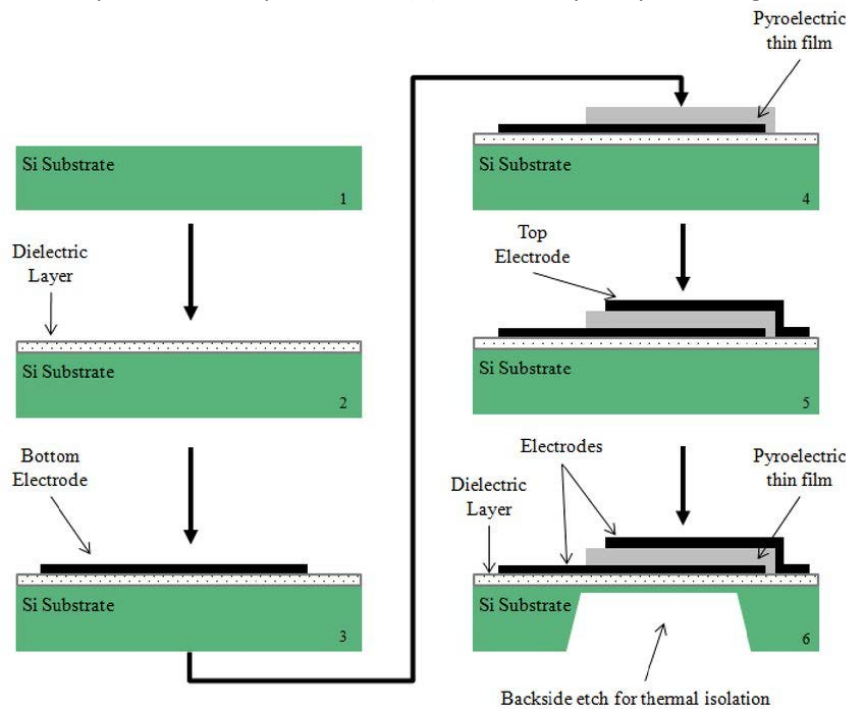


**Figure 6** illustrates all of the steps performed during the fabrication process.

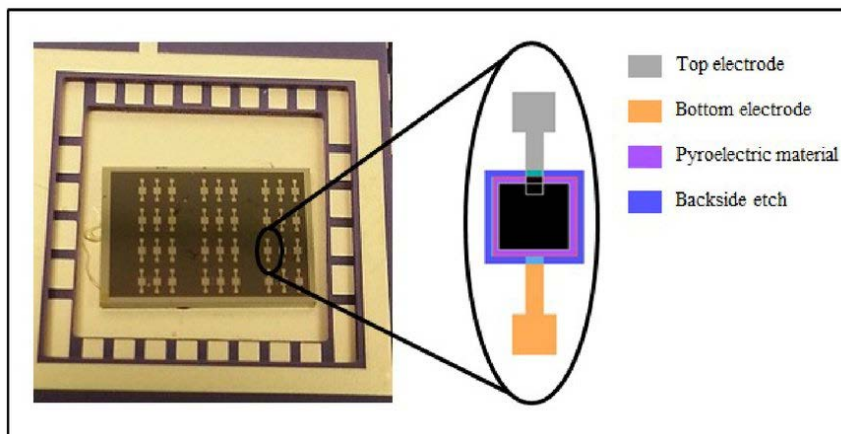
**Figure 6.** Step by step methodology used to fabricate the pyroelectric test structures. A dielectric layer is deposited on a bare Si wafer (2). Next, the first mask is used to pattern the bottom electrode (3). The second mask is used to pattern the pyroelectric film after the deposition of the bottom electrode (4). The third mask is used to pattern the top electrode (5) followed by the patterning of the backside etch using the fourth mask (6).



#### 4. TESTING

Once all of the steps were completed in the fabrication process, the processed wafers were ready to be tested. However, for the test configuration used in this research, the wafers were diced into smaller samples and mounted to carriers using crystal bond, and wire-bonded for ease of measuring the pyroelectric voltage response. **Figure 7** shows a sample with 36 devices mounted to a carrier before being wire-bonded.

**Figure 7.** Pyroelectric devices mounted on a carrier ready for wire-bonding. A close up view of one of the 36 devices is shown.

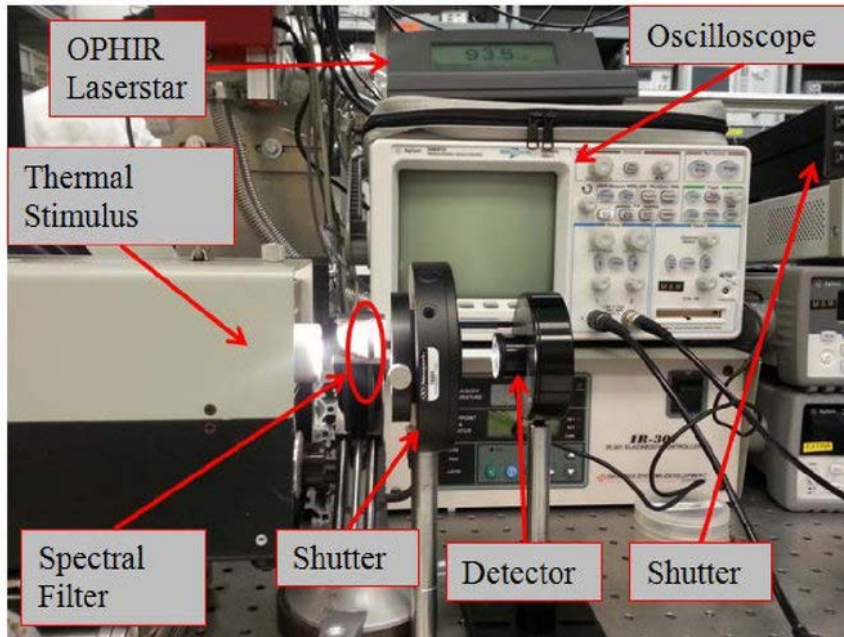


An MKII Fiber optic light was used as an energy source to provide thermal stimulus to the pyroelectric material. The thermal stimulus was chopped using a UNIBLITZ® T132 Shutter driver and shutter. The pyroelectric voltage response was measured across the Au electrodes using an Agilent 54641D Mixed



Signal Oscilloscope. The distance of the MKII Fiber optic light aperture to the pyroelectric devices was four inches during testing. After the test configuration was complete, the wire-bonded pyroelectric devices and place the carrier they were housed in were placed onto a breadboard and the devices were connected in parallel to create a larger sensing area, with the goal of removing the connected devices one at a time to determine the pyroelectric voltage response of an individual device. The test configuration can be seen in **Figure 8**.

**Figure 8.** The test configuration for measuring the pyroelectric voltage response consists of the energy source, power detector, filter, shutter, oscilloscope, and angle bracket holding the pyroelectric device.

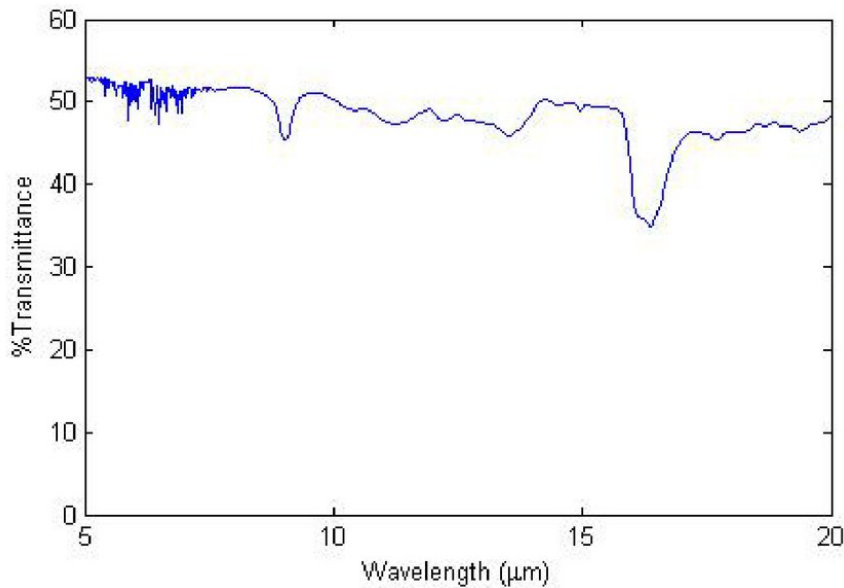


## 5. RESULTS

The pyroelectric voltage response of several  $300 \times 300 \mu\text{m}^2$  area square devices was measured using the test setup shown in **Figure 8**. The incident power was measured to be 81.4 mW without a filter, 6.8 mW with the Si filter, and 5.0 mW with the Oriel 59562 long pass filter at a distance of four inches onto a spot size of  $1.27 \text{ cm}^2$ . The shutter frequency was set to 1 Hz for all of the measurements.

As stated above, the pyroelectric voltage response of the square pyroelectric devices was measured. The individual devices were wire bonded and two of them were connected in parallel using a breadboard. The breadboard was placed in the angle bracket at the pre-determined distance of four inches (this is where the incident power of 81.4 mW was measured) away from the light source. The pyroelectric voltage responses were measured with both of the devices connected; without a filter, with a Si filter and with an Oriel 59562 long pass filter. The Si filter had a transmittance of approximately 46 – 50% from  $1.1 \mu\text{m}$  to  $20 \mu\text{m}$  allowing for pyroelectric voltage response measurements in the infrared (IR) region. The transmittance of the double-sided polished Si from  $5 \mu\text{m}$  to  $20 \mu\text{m}$  can be seen in **Figure 9**.

**Figure 9.** Transmittance of a double-side polished Si sample to be used as a filter. This filter is used to filter out wavelengths below 1.1  $\mu\text{m}$  in order to allow for pyroelectric voltage response measurements in the IR region.



The Oriel 59562 long pass filter is a commercial filter and has a transmittance of approximately 100% in the 1 – 2.6  $\mu\text{m}$  region. This long pass filter was used to filter out the wavelengths below 1  $\mu\text{m}$  and above 3  $\mu\text{m}$  in order to allow for the pyroelectric voltage response to be measured in the short wavelength IR (SWIR) region. The transmittance plot for this filter can be found in the Oriel Instruments technical specifications sheet.

**Figure 10** shows a measured pyroelectric voltage response of 38.9  $\text{mV}_{\text{p-p}}$  from the two-pyroelectric device configuration without any filtering.

**Figure 10.** Pyroelectric voltage of 2 square devices without any filtering.

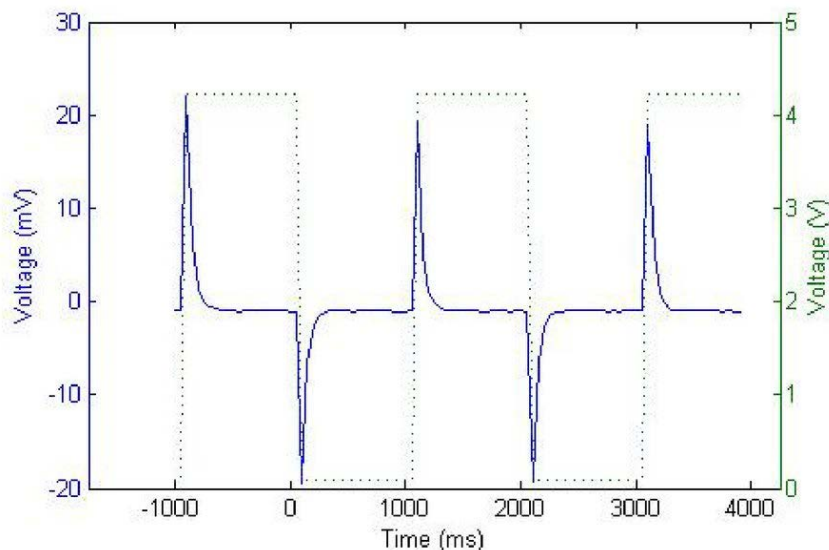


**Figure 11** shows a measured pyroelectric voltage response of 12.45  $\text{mV}_{\text{p-p}}$  in the IR region from the two-pyroelectric device configuration with 9.63  $\mu\text{W}$  of incident power on the devices.



**Figure 11.** Pyroelectric voltage of 2 square devices using a Si filter.

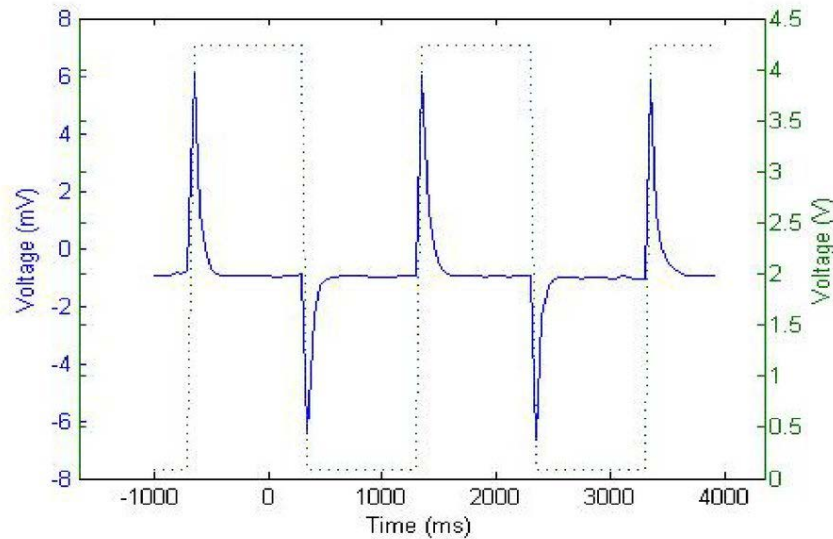
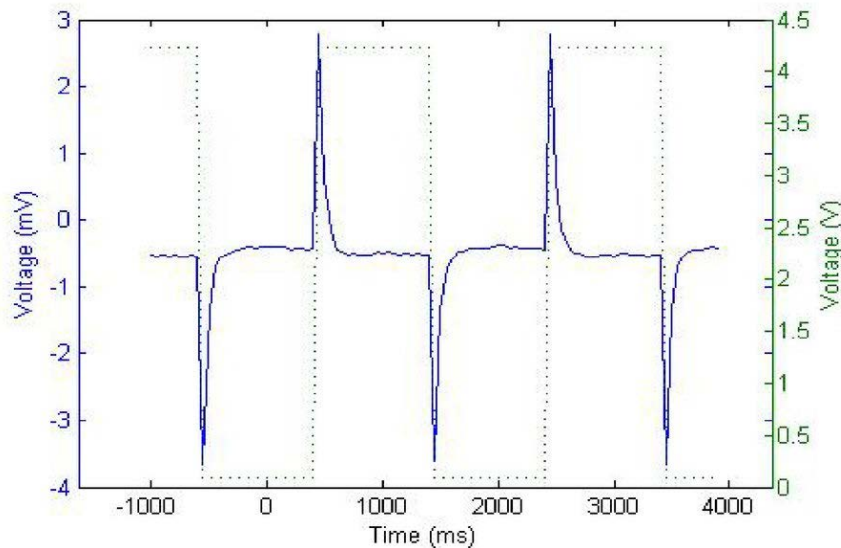


**Figure 12** shows a measured pyroelectric voltage response of  $6.38 \text{ mV}_{p-p}$  in the SWIR from the two-pyroelectric device configuration with  $7.087 \mu\text{W}$  of incident power on the devices.

**Figure 12.** Pyroelectric Voltage of 2 square devices using an Oriel 59562 long pass filter.



## 6. CONCLUSIONS

Using MEMS fabrication techniques pyroelectric devices were created that allowed for the measurement of the pyroelectric voltage response of AlN. The results show that the pyroelectric properties of AlN were sensitive to thermal stimulus over a wide spectral range and to the wavelengths in the IR and SWIR regions. These results also show that this MEMS pyroelectric device, with AlN as the pyroelectric material, can be utilized in sensing applications.

## ACKNOWLEDGEMENTS

The authors would like to thank the Air Force Research Laboratory (AFRL) Sensors Directorate for their assistance, use of their resources, and facilities. The authors also thank the technical support and dedicated work of AFIT's own cleanroom staff, Mr. Rich Johnston and Mr. Thomas Stephenson and

Physics Department laboratory technician Mr. Michael Ranft. Lastly, the authors would like to thank AFRL's John Goldsmith for sputtering AlN thin-films used for this research.

**Disclaimer:** The views expressed in this article are those of the authors and do not reflect the official policy or position of the United States Air Force, Department of Defense, or the United States Government.

## REFERENCES

- [1] J. Cooper, "Minimum detectable power of a pyroelectric thermal receiver," AIP Review of Scientific Instruments, vol. 33, no. 1, pp. 92–95, 1962. **10.1063/1.1717673**
- [2] X. Ding-Quan and S. B. Lang, "Measurement Applications Based on Pyroelectric Properties of Ferroelectric Polymers," IEEE Transactions on Electrical Insulation, vol. 23, no. 3, pp. 503–516, 1988. Google Scholar
- [3] S. B. Lang, "Pyroelectricity: From Ancient Curiosity to Modern Imaging Tool," Physics Today, pp. 31–36, 2005. **10.1063/1.2062916**
- [4] A. Rogalski, Infrared Detectors, Amsterdam: Gordon and Breach Science Publishers, 2000. Google Scholar
- [5] W. S. Yan, R. Zhang, X. Q. Xiu, Z. L. Xie, P. Han and et. al., "Temperature dependence of the pyroelectric coefficient and the spontaneous polarization of AlN," AIP Applied Physics Letters, vol. 90, pp. 212102-1 – 212102-3, 2007. Google Scholar
- [6] S. T. Liu and D. Long, "Pyroelectric Detectors and Materials," Proceedings of the IEEE, vol. 66, no. 1, pp. 14–26, 1978. Google Scholar
- [7] G. S. May and S. M. Sze, Fundamentals of Semiconductor Fabrication, Hoboken, New Jersey: John Wiley & Sons, Inc., 2004. Google Scholar